A Search for Exotic S=-2 Baryons Decaying to $\Xi^{\pm}\pi^{\pm}$

Text for the blessed web page – CDF note 6855

The CDF Collaboration

March 3, 2004

Abstract

Using Ξ tracks reconstructed in CDF Silicon detector we have performed search for these states using $\sim$ 220 pb^{-1} of data collected with two track trigger. No signal was found and we obtained the following upper limits in the numbers of events:

Channel	UL 90 % CL	UL 95 % CL
$\Xi^-\pi^+$	126	144
$\Xi^-\pi^-$	51	63

The relative yields with respect to well established resonance $\Xi(1530)$ were found to be:

Channel	UL 90 % CL	UL 95 % CL
$\Xi^-\pi^+$	0.06	0.07
$\Xi^-\pi^-$	0.03	0.04

In order to verify that TTT sample does not inroduce significant bias that adversly impact pentaquark acceptance the we have search for these states in JET20 data using comprising 220 pb^{-1} of integrated luminosity. No signals were observed.

The clean sample of Ξ tracks in TTT data is about 18 times larger than the sample that NA49 has, while JET20 sample is twice as large.

1 Introduction

An observation of manifestly exotic S=-2 baryon states decaying to $\Xi^{\pm}\pi^{\pm}$ [1] in proton-proton collisions of CERN SPS at $\sqrt{s} = 17.2$ GeV has recently been reported by NA49 Collaboration [1]. The observed states, or to be precise the double negative state, could not be described as three-quark states and were interpreted as $I_3 = -\frac{3}{2}$ and $I_3 = +\frac{1}{2}$ partners of isospin quadruplet of five-quark states, pentaquarks, with quark contents $(dsds\bar{u})$ and $(dsus\bar{d})$ correspondingly. The combined mass of $\Xi^{--}_{3/2}$ and $\Xi^{0}_{3/2}$ was measured to be (1.862 ± 0.002) GeV/c^2.

The NA49 result complemented a number of observations of an exotic S=+1 baryonic state in NK channel, the Θ^+, claimed recently by various experiments [2-7]. The Θ^+ state and the $\Xi^{--,0}_{3/2}$ states are believed to belong to the minimal pentaquark anti-decuplet, depicted in Figure 1.

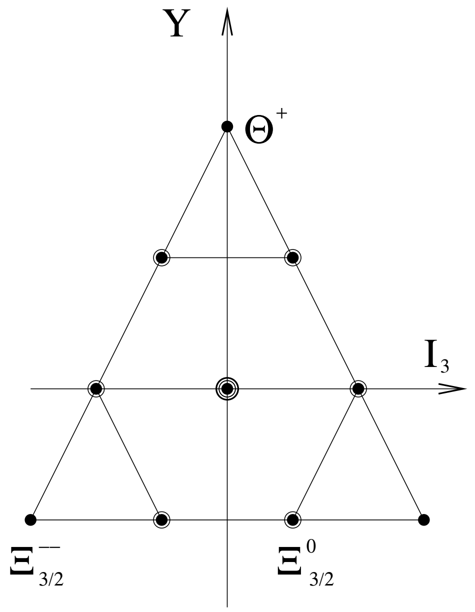

Figure 1: Pentaquark multiplets - $\mathbf{\bar{10}}_f + \mathbf{8}_f$

All results are based on relatively low statistics samples with 20 – 100 events in peaks and estimated significance in the range from 3 to 5.

The news about presence of narrow state in the $\Xi\pi$ invariant mass spectrum was very surprising as this spectrum has been looked at by several generations of fixed target experiments without a single claim at the bump at the mass observed by NA49. For excellent review of the available experimental data in the context of recent pentaquark observations see [9].

At CDF we recently developed a technique of hyperon tracking in the silicon detector. The hyperon tracking allows to obtain superior momentum and vertex resolution of Ξ with respect to conventional technique of using Ξ decay products to measure its momentum and

[1] Unless otherwise noted all references to the specific charge combination imply charge conjugate combination as well

decay vertex; as well as to significantly reduce combinatorial background. The CDF note 6527 describes the hyperon tracking in detail [10]. We intended to use hyperons, tracked in the Silicon detector, to reconstruct bottom-strange baryons $\{\Xi_b^-, \Xi_c^0\}$. Bottom-strange baryons decay predominantly to charmed-strange baryons $\{\Xi_c^0, \Xi_c^+\}$ which in turn decay to Ξs and a number of pions. We were able to reconstruct $\Xi_c^0 \to \Xi^-\pi^+$ applying cuts tailored for Ξ_b reconstruction. Clear signal from well established resonance $\Xi(1530)$ has been observed as well. See note 6527 for details. No peaks were seen in the mass region of 1.860 GeV/c^2, though this region is not shown in the plots presented in [10].

Observation of peaks at 1.860 GeV/c^2 in $\Xi^-\pi^+$ and $\Xi^-\pi^-$ invariant mass spectra reported by NA49 prompted more careful study of these spectra at CDF. Of special interest was $\Xi^-\pi^-$ as we did not analyze this charge combination previously.

2 TTT data

The inclusive sample of SVX Ξ tracks was selected from two available B-hadronic datasets – hbhd08 and hbhd09. The events were required to pass `B_CHARM*` triggers. The corresponding integrated luminosity is about 220 pb^{-1}, no run quality selection has been applied. The invariant mass spectrum of $\Lambda\pi^-$ combinations is presented in Figure 2. The number of events is 36,000.

The invariant mass of $\Xi\pi^+$ pairs is represented by points with error bars in Figure 3, a filled histogram shows $\Xi\pi^-$ combinations. A prominent peak corresponding to the decay $\Xi(1530) \to \Xi\pi^+$ is visible in the $\Xi\pi^+$ mass spectrum. The pentaquark mass is marked with an arrow. Apparently no signal is visible in either distribution.

Fit to non-relativistic Breit-Wigner convoluted with Gaussian resolution function with natural width fixed to the known PDG value, $\Gamma(\Xi(1530)) = 9.1$ MeV/c^2, yielded results summarized in Table 1 1.

χ^2/ndf	52/66
yield	$2,182 \pm 92$
Mass	$(1,532 \pm 4)$ MeV/c^2
Gaussian σ	(5.8 ± 0.5) MeV/c^2

Table 1: The results of the fit to the $\Xi\pi^+$ invariant mass distribution in TTT data

Figure 4 b) shows what is observed at CDF. Superimposed function shows fit with the Gaussian and 3-rd order polynomial. The width and the means of Gaussian were fixed to 8 MeV/c^2 1.862 GeV/c^2 correspondingly. Fit yielded (47 ± 70) events.

We presented $\Xi\pi^\pm$ spectrum shown in Figure 4 for better comparison with NA49 [1] who chose to combine $\Xi(1860)^{--}$ and $\Xi(1860)^0$ states into one result. But as these are indeed two states, possibly with different masses due to isospin splitting and different production rates due to different quark content, we present the results for each state separately. Figures 5 a),b) show $\Xi^-\pi^+$ and $\Xi^-\pi^-$ spectra correspondingly.

The upper limits on the number of observed events in the region of pentaquark mass were obtained by performing a series of fits to each of the distribution with all parameters of Gaussian describing pentaquark fixed, scanning its amplitude with step=1 from -2000 to 2000. For each fit a likelihood is extracted and resulting likelihood profile vs number of signal events is obtained. Numbers N at which there are 90% and 95% of profile integral calculated over positive N correspond to 90% and 95% Confidence Level upper limits. Fits to $\Xi\pi^{\pm}$ did not include the region of $\Xi(1530)$ resonance.

The upper limits on the number of events are summarized in Table 2

Channel	# of events	UL 90 % CL	UL 95 % CL
$\Xi^-\pi^+$	57 ± 51	126	144
$\Xi^-\pi^-$	-54 ± 47	51	63
$\Xi^-\pi^{\pm}$	47 ± 70	150	176

Table 2: Upper limits on the number of events in $\Xi(1860)$ mass region in TTT sample

And upper limits on relative yields are broken down in Table 3.

yield	UL 90 % CL	UL 95 % CL
$r^0_{\rm CDF}$	0.06	0.07
$r^{--}_{\rm CDF}$	0.03	0.04
$r_{\rm CDF}$	0.07	0.08

Table 3: Upper limits on the relative yields of $\Xi(1860)$ in TTT data

Where raw relative yields are defned as the rations of event numbers.

The production mechanism of pentaquarks is unknown. The TTT sample is enhanced with b and c-hadron decays that may introduce a bias that adversely affects detector acceptance for pentaquark states. We cross checked our results by repeating analysis on JET20 trigger data.

3 The JET20 Trigger Data

The invariant mass of $\Xi\pi^+$ pairs is represented by points with error bars in Figure 7, the filled histogram shows $\Xi\pi^-$ combinations. Statistically significant corresponding to the decay $\Xi(1530) \to \Xi\pi^+$ is visible in the $\Xi\pi^+$ mass spectrum. The pentaquark mass is marked with an arrow. Apparently no signal is visible in either distribution.

A fit to non-relativistic Breit-Wigner convoluted with Gaussian resolution function with natural width fixed to the value obtained from TTT data and known PDG value correspondingly yielded the following results:

χ^2/ndf	111/88
yield	387 ± 34
Mass	$(1,5323 \pm 0.8)$ MeV/c^2
Gaussian σ	5.8 (fixed)

Table 4: Results of the fit to $\Xi\pi^+$ invariant mass distribution for JET20 data

Figure 8 shows $\Xi\pi^{+-}$ invariant mass spectrum. Superimposed function shows fit with the Gaussian and 3-rd order polynomial. $\Xi(1530)$ region was excluded from the fit for simplicity. The width and the mean of Gaussian were fixed to 8 MeV/c^2 1.862 GeV/c^2 correspondingly. Fit yielded (-16 ± 27) events. Figures 9 a,b show separately $\Xi^-\pi^+$ and $\Xi^-\pi^-$ spectra. The upper limits on the number of events are summarized in table 5

Channel	# of events	UL 90 % CL	UL 95 % CL
$\Xi^-\pi^+$	-14 ± 19	25	30
$\Xi^-\pi^-$	-4 ± 18	28	33
$\Xi^-\pi^\pm$	-16 ± 27	35	43

Table 5: Upper limits on the number of events in $\Xi(1860)$ mass region in JET20 sample

And upper limits on relative yields:

yield	UL 90 % CL	UL 95 % CL
r^0_{CDF}	0.06	0.08
r^{--}_{CDF}	0.07	0.09
r_{CDF}	0.09	0.11

Table 6: Upper limits on the relative yields of $\Xi(1860)$ in JET20 data

References

[1] C. Alt *et al.* [NA49 Collaboration], arXiv:hep-ex/0310014.

[2] T. Nakano *et al.* [LEPS Collaboration], Phys. Rev. Lett. **91**, 012002 (2003) [arXiv:hep-ex/0301020].

[3] V. V. Barmin *et al.* [DIANA Collaboration], Phys. Atom. Nucl. **66**, 1715 (2003) [Yad. Fiz. **66**, 1763 (2003)] [arXiv:hep-ex/0304040].

[4] J. Barth *et al.* [SAPHIR Collaboration], Phys. Lett. B **572** (2003) 127.

[5] A. E. Asratyan, A. G. Dolgolenko and M. A. Kubantsev, arXiv:hep-ex/0309042.

[6] V. Kubarovsky *et al.* [CLAS Collaboration], arXiv:hep-ex/0311046.

[7] A. Airapetian *et al.* [HERMES Collaboration], arXiv:hep-ex/0312044.

[8] Particle Data Group, K. Hagiwara *et al.*, Phys. Rev. **D 66**, 2002

[9] H. G. Fischer and S. Wenig, arXiv:hep-ex/0401014.

[10] E.A. Gerchtein, D.O. Litvintsev, P.T. Lukens "Tracking of Hyperons in SVX detector" CDF/PUB/TRACKING/PUBLIC/6527

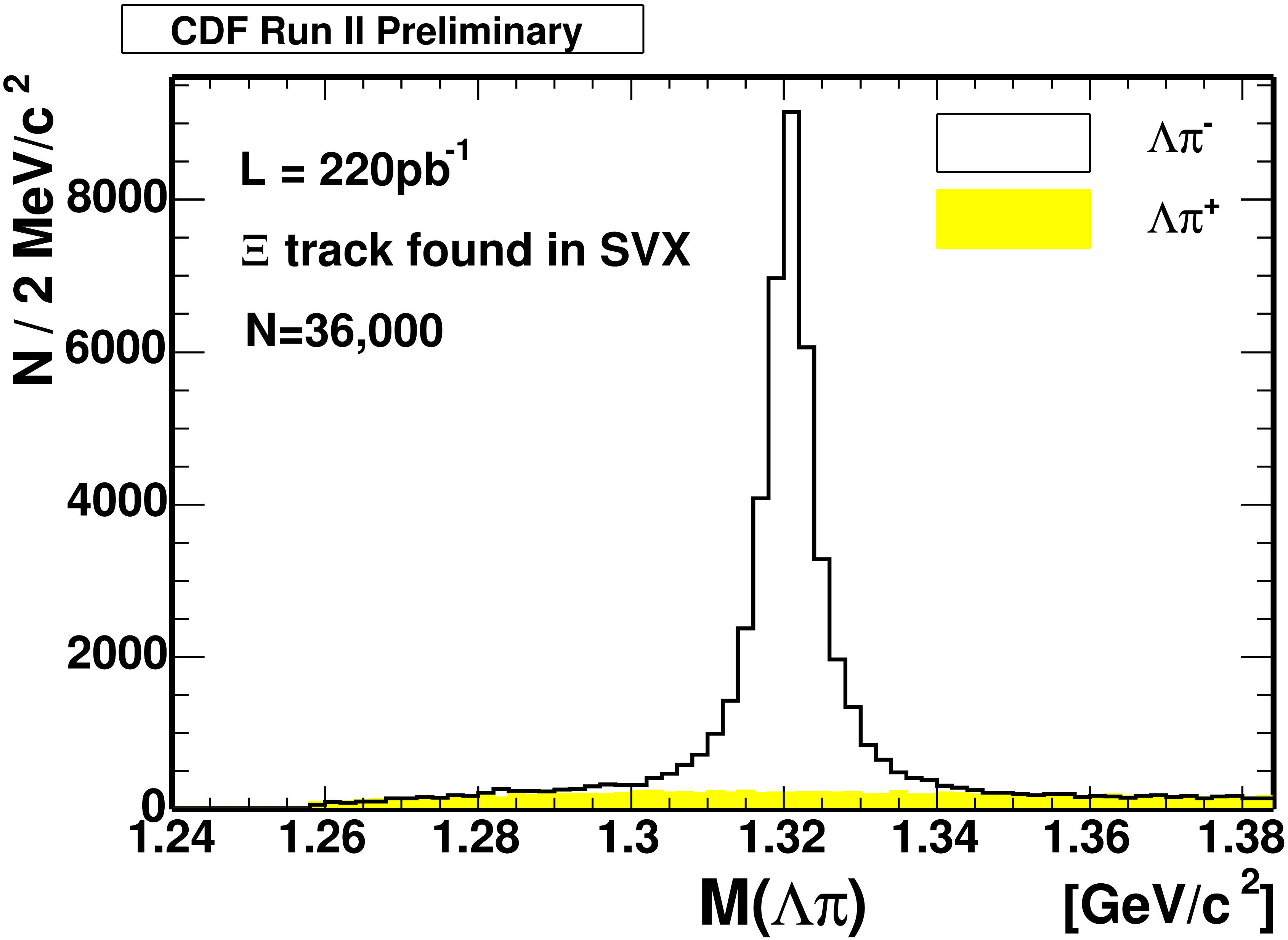

Figure 2: An invariant mass spectrum of $\Lambda\pi$ combinations in TTT sample after requiring at least 2 $r-\phi$ SVX hits on Ξ track. An open histogram shows right sign $\Lambda\pi^-$ combinations; the filled histogram shows wrong sign $\Lambda\pi^+$ combinations.

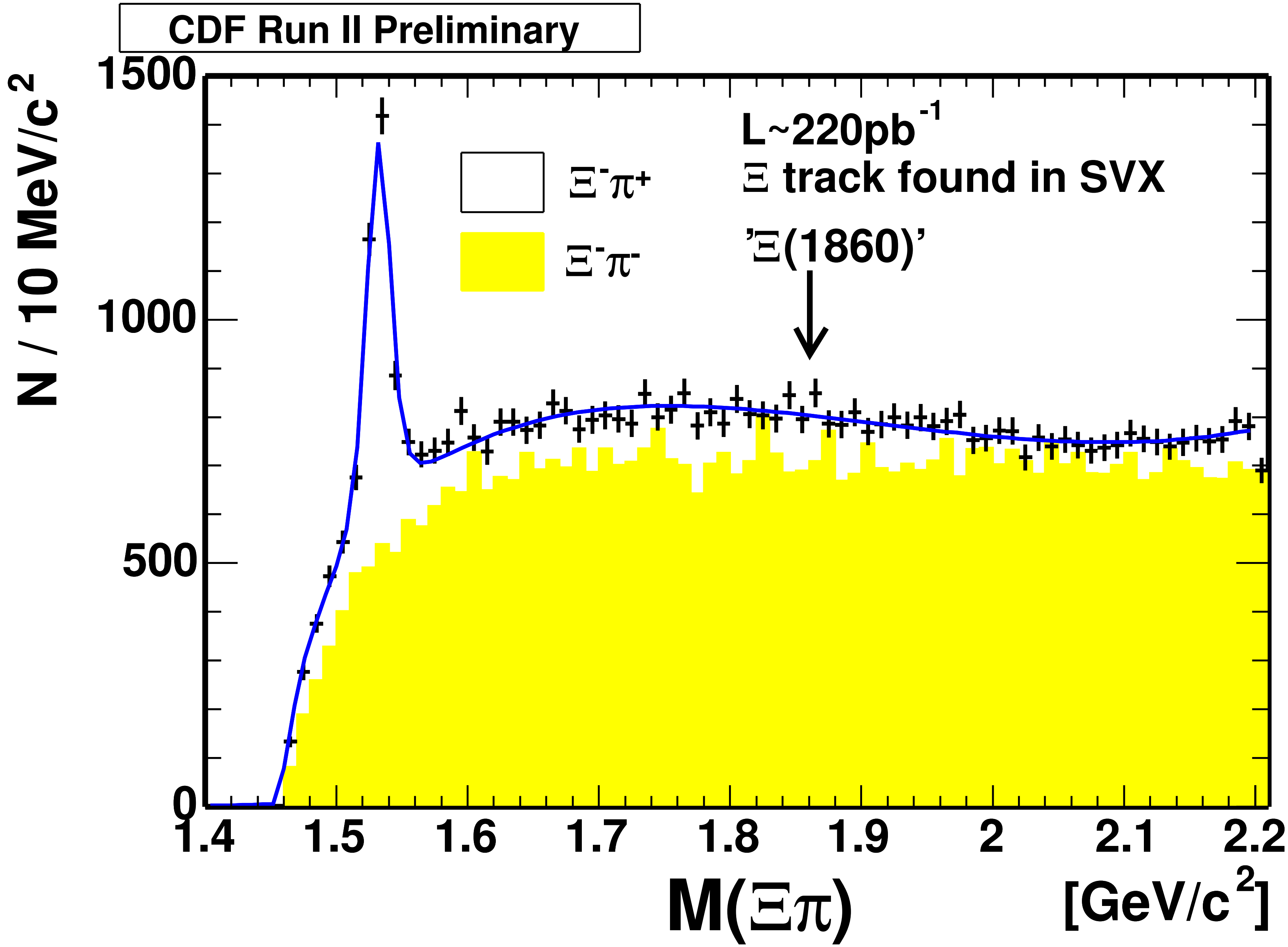

Figure 3: $\Xi\pi^+$ invariant mass distribution (points with error bars) and wrong sign – $\Xi\pi^-$ (filled histogram)

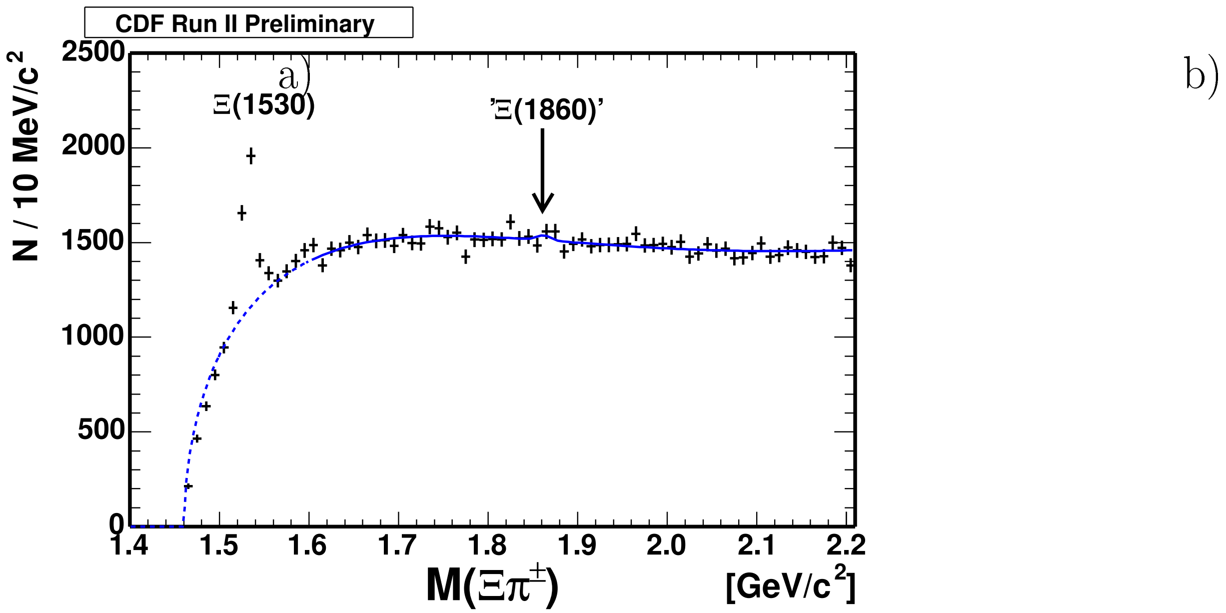

Figure 4: Invariant mass spectrum of $\Xi\pi^{\pm}$ combinations

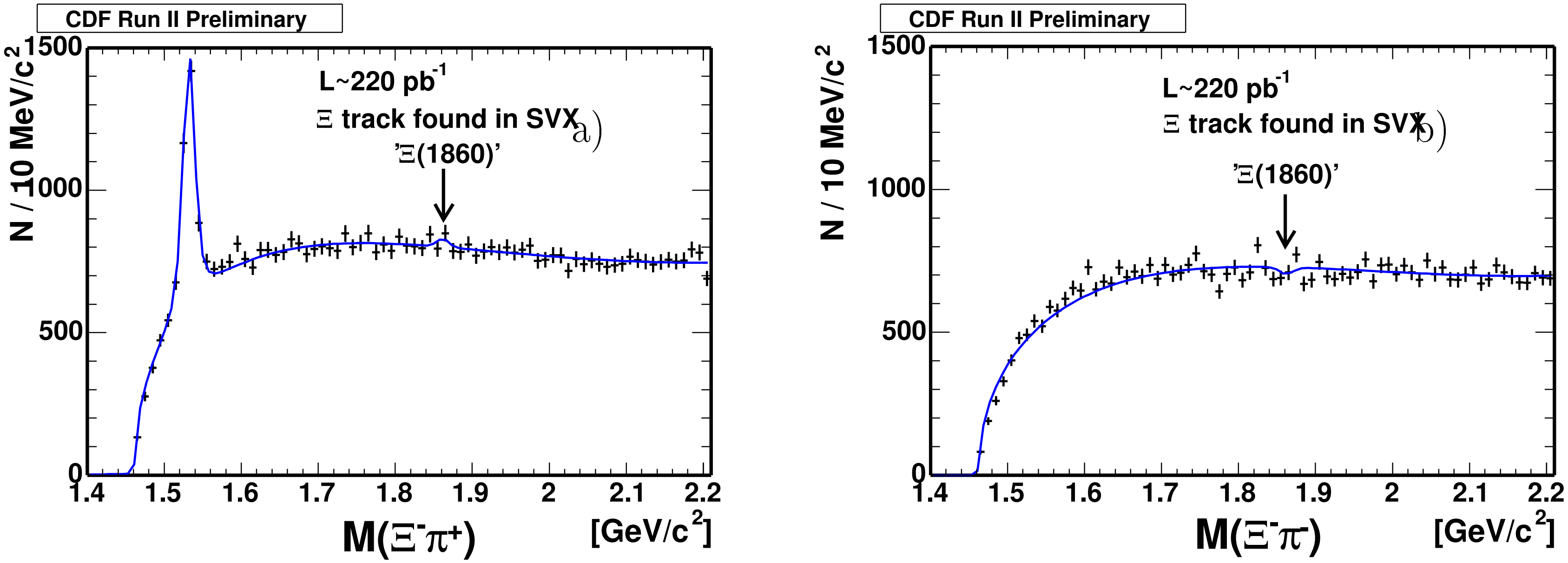

Figure 5: a) $\Xi^-\pi^+$ invariant mass spectrum; b) $\Xi^-\pi^-$ invariant mass spectrum. Superimposed functions show results of the fits described in the text.

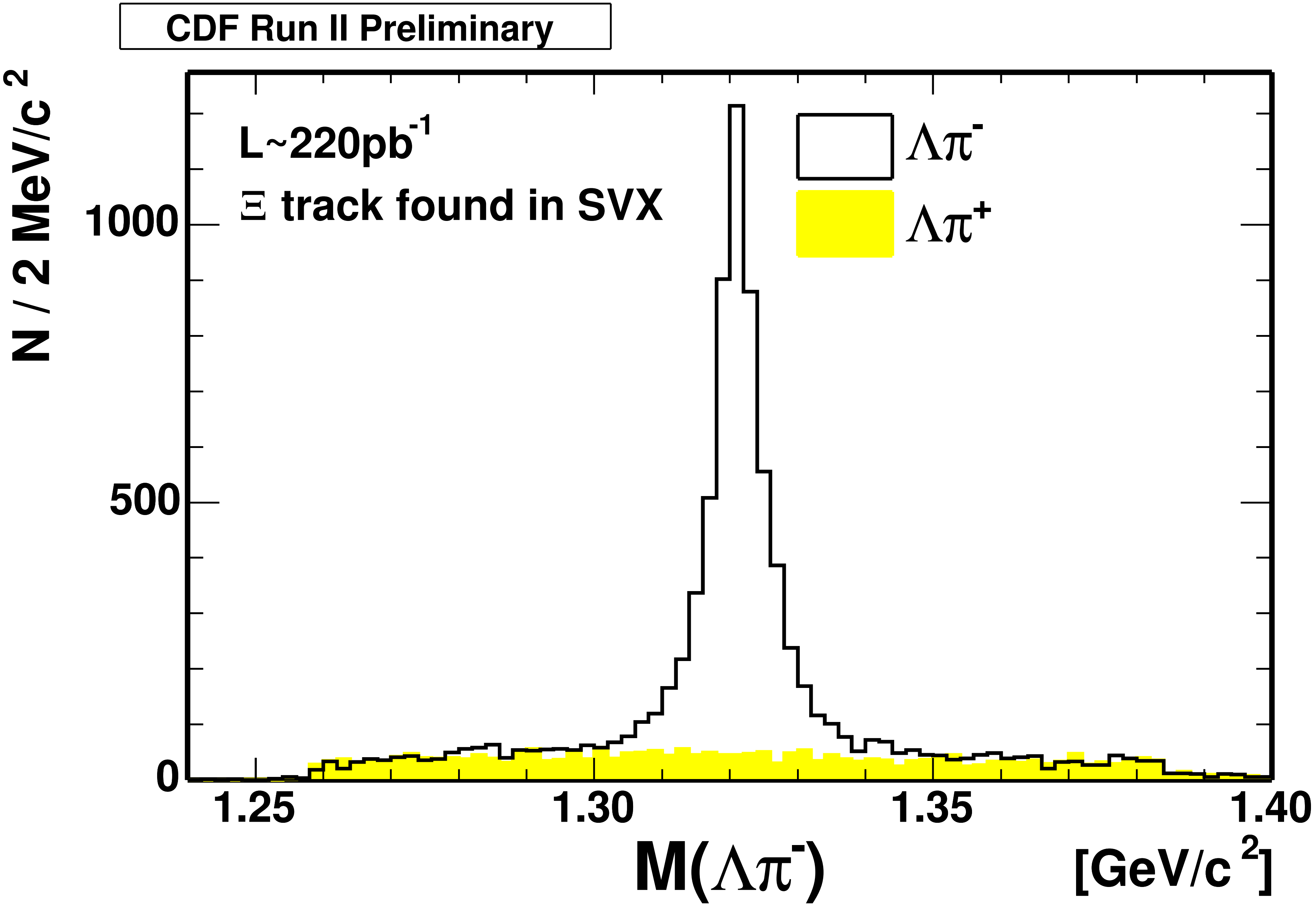

Figure 6: The $\Lambda\pi^-$ invariant mass distribution (open histogram), wrong sign – $\Lambda\pi^+$ (filled histogram)

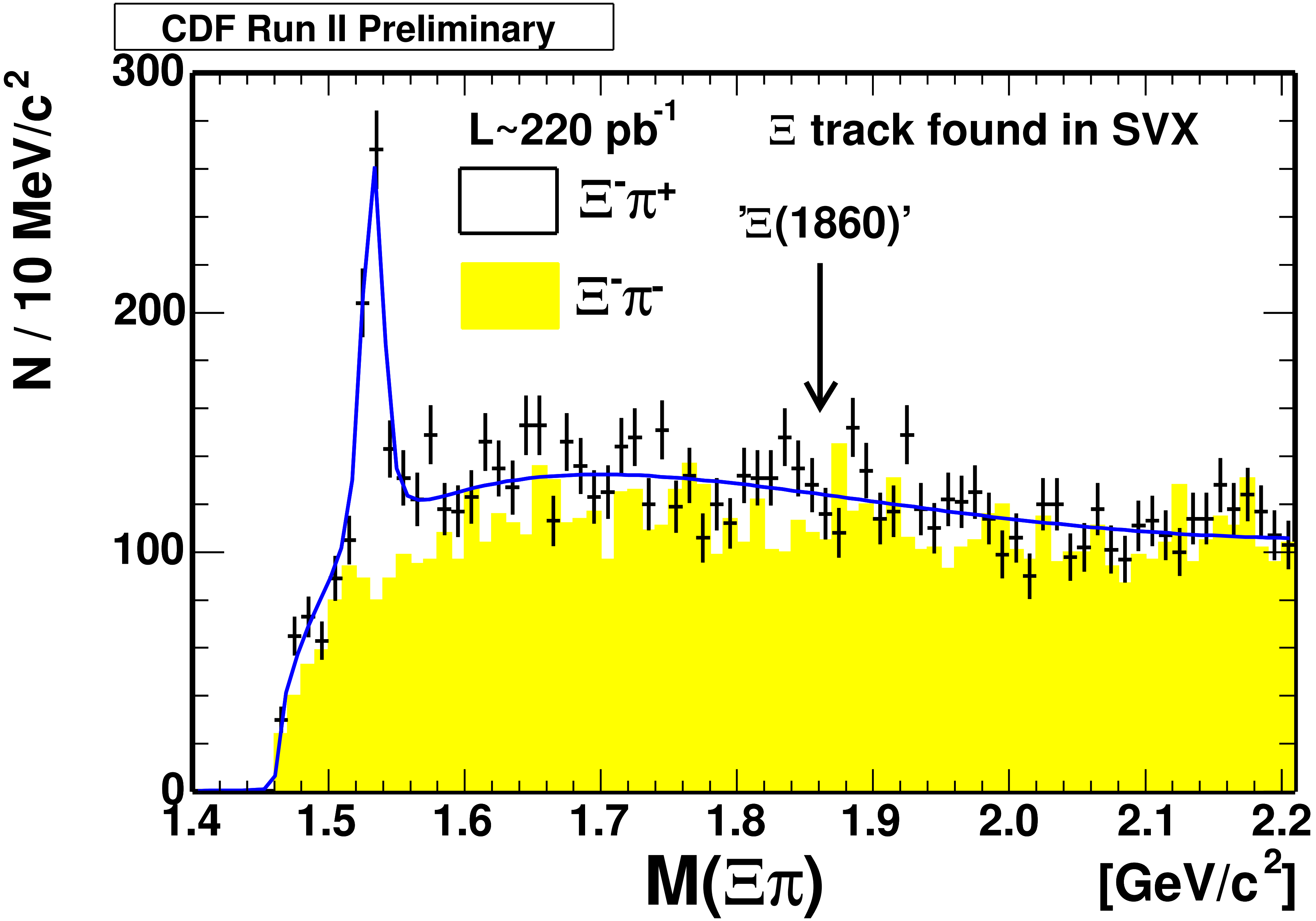

Figure 7: JET 20 Data. $\Xi\pi^+$ invariant mass distribution (points with error bars) and wrong sign – $\Xi\pi^-$ (filled histogram)

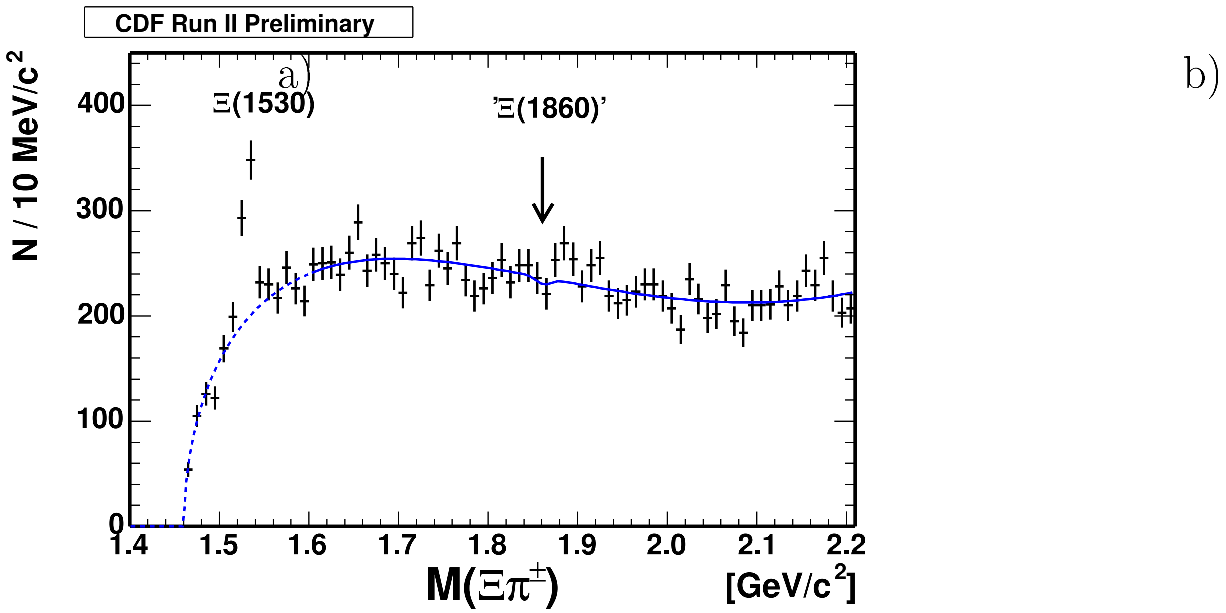

Figure 8: Invariant mass spectrum of $\Xi\pi^{\pm}$ combinations

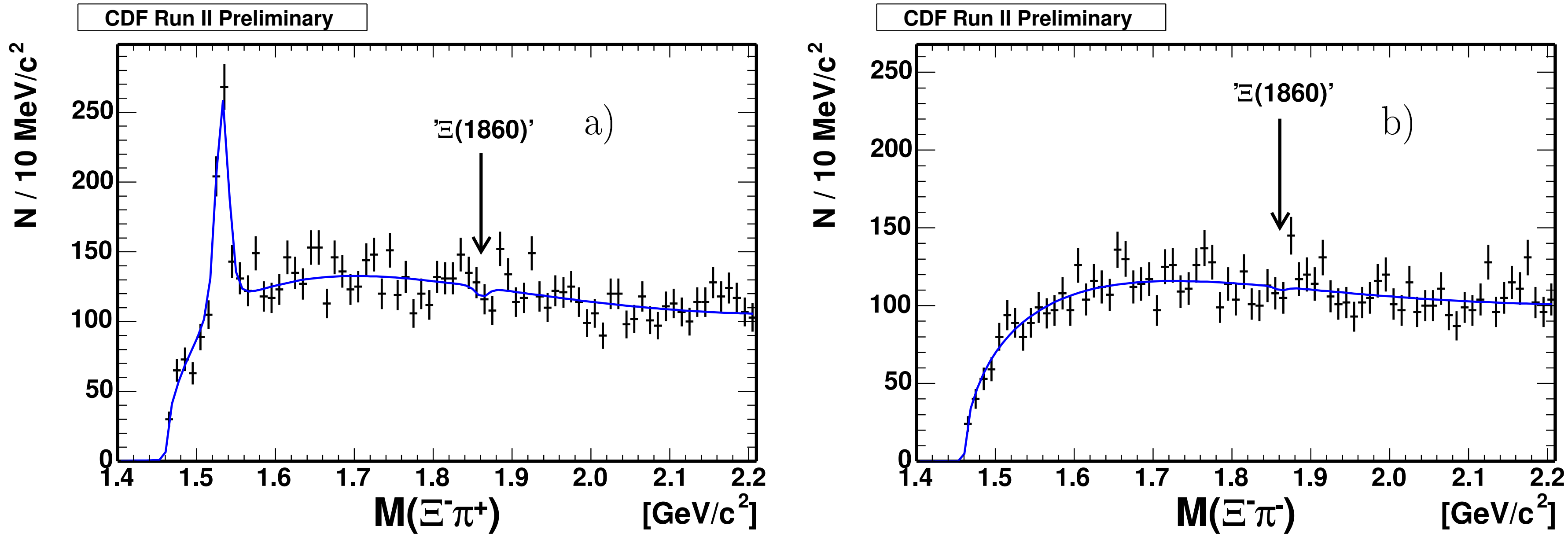

Figure 9: JET20 data; a) $\Xi^{-}\pi^{+}$ invariant mass spectrum; b) $\Xi^{-}\pi^{-}$ invariant mass spectrum. Superimposed functions show results of the fits described in the text.

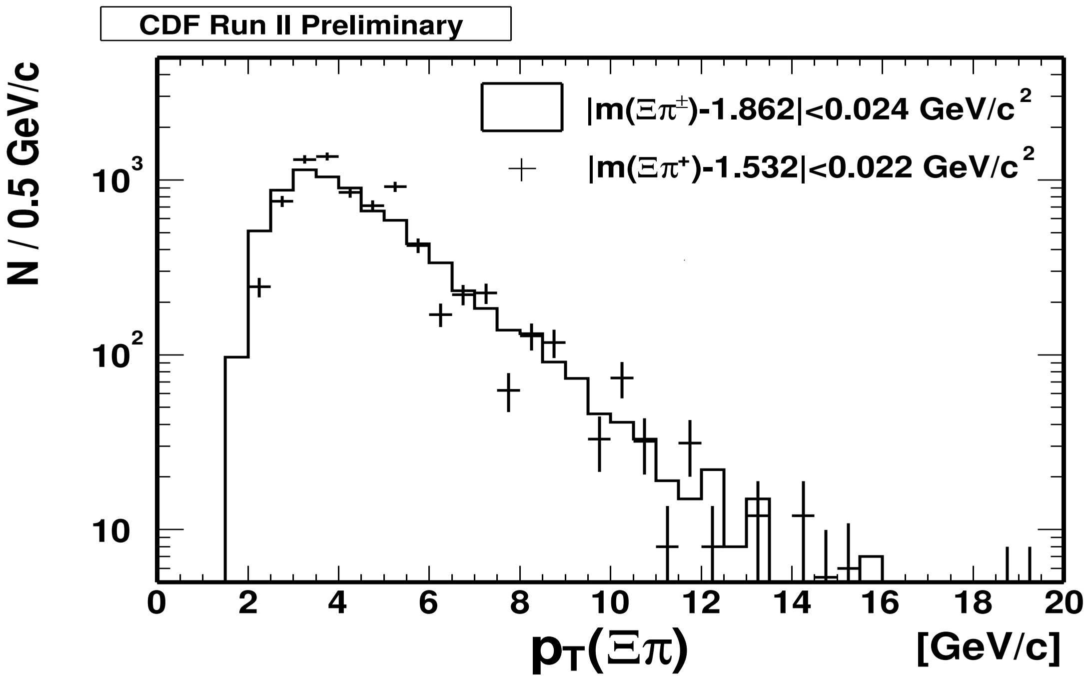

Figure 10: The p_T spectrum of $\Xi\pi^{\pm}$ combinations with an invariant mass in the pentaquark signal region (solid line histogram). Points with error bars show the p_T of $\Xi(1530)$. The latter histogram is scaled to have the same integral as the former.

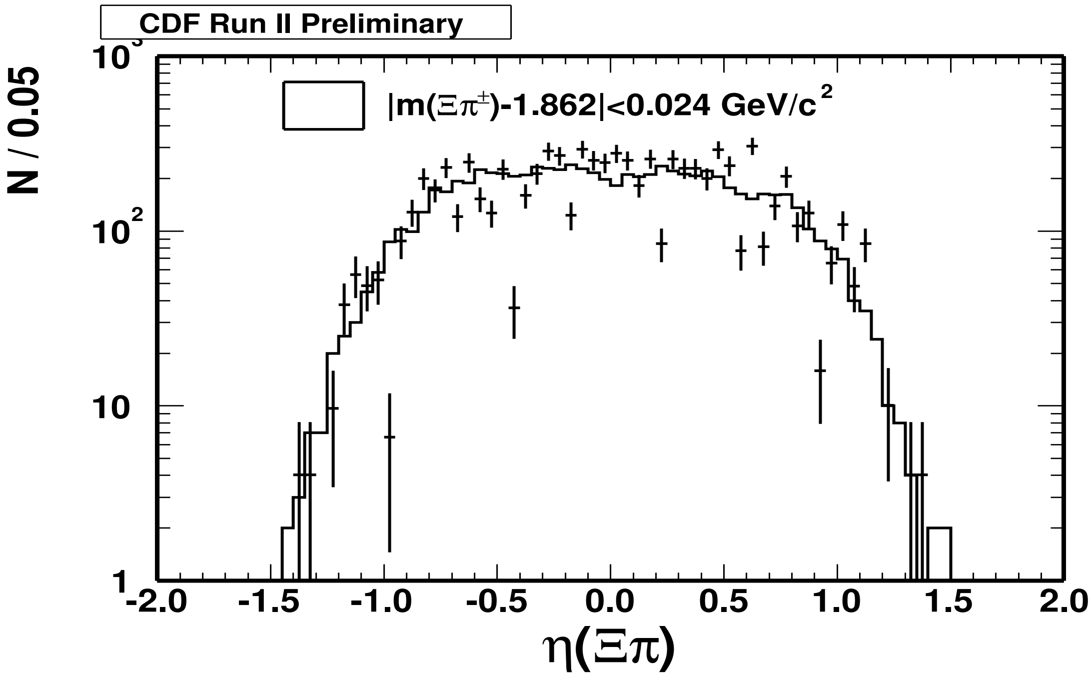

Figure 11: The η spectrum of $\Xi\pi^{\pm}$ combinations with an invariant mass in the pentaquark signal region (solid line histogram). Points with error bars show the η of $\Xi(1530)$. The latter histogram is scaled to have the same integral as the former.

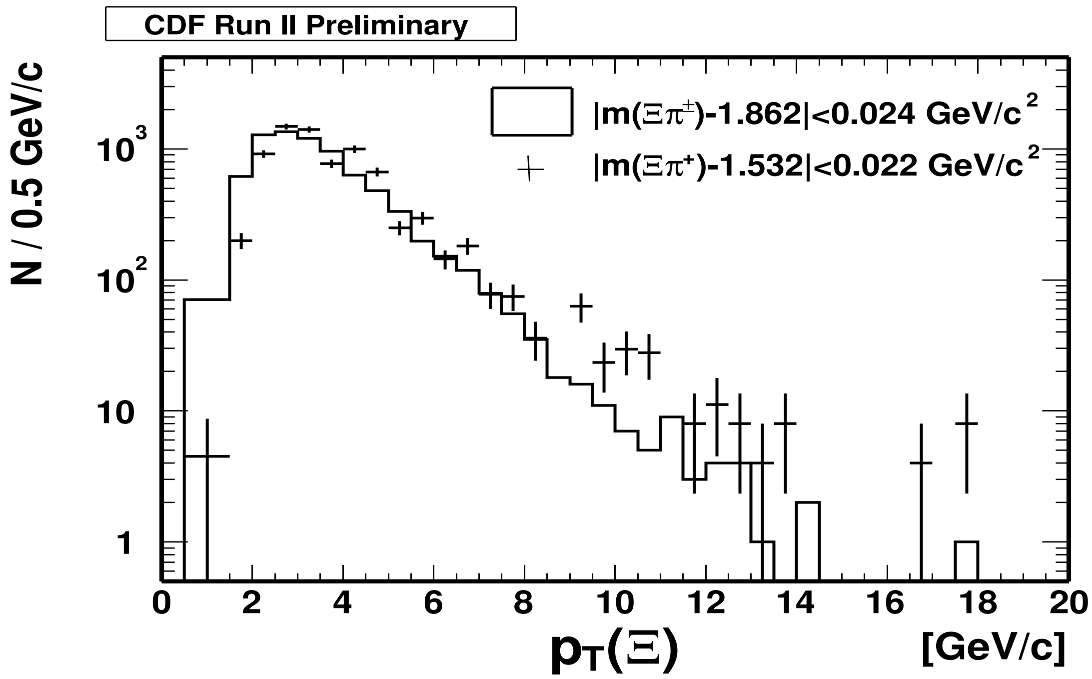

Figure 12: The p_T spectrum of Ξ tracks for $\Xi\pi^\pm$ pairs from pentaquark mass region (open histogram). Points with error bars show the p_T of $\Xi(1530)$. The latter histogram is scaled so both histograms have the same integral.

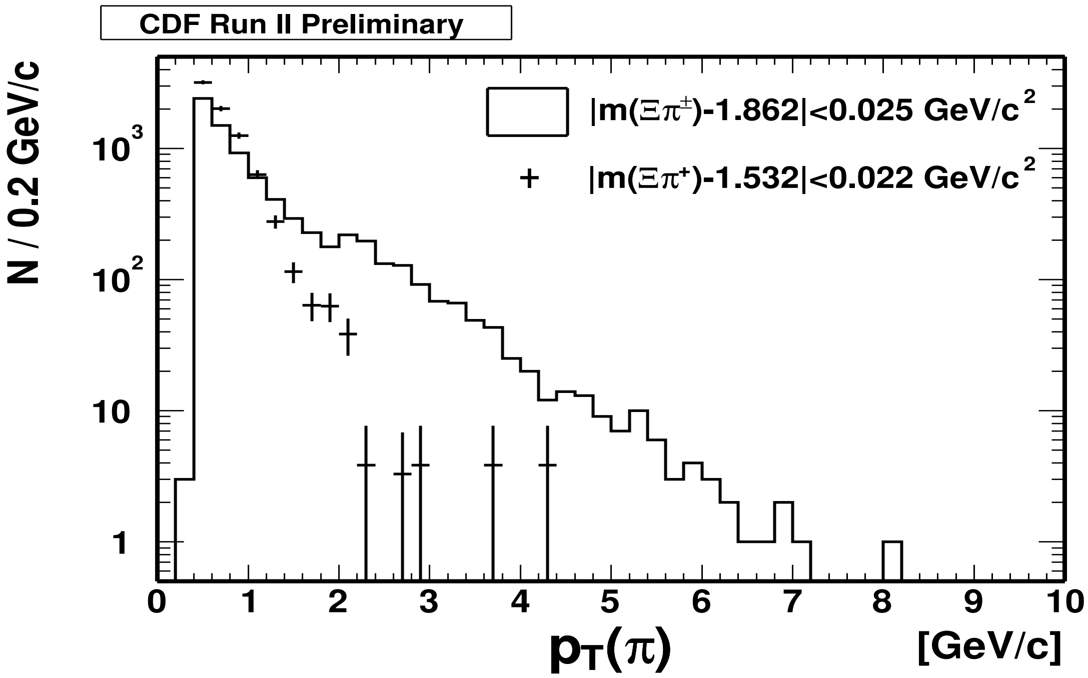

Figure 13: The p_T spectrum of π of $\Xi\pi^{\pm}$ pairs in pentaquark mass region (open histogram). Points with error bars shows scaled p_T spectrum of $\Xi(1530)$. It is clear that pions from $\Xi(1530)$ decays are significantly softer as $\Xi(1530)$ has a mass close to $\Xi\pi$ threshold.